INTERNATIONAL JOURNAL OF MICROWAVE AND OPTICAL TECHNOLOGY,
VOL.19, NO.6, NOVEMBER 2024

Design and Development of Circular Patch MIMO Antenna for Commercial Applications

Srinivas Padala[*1], Dr. Arun Raaza[1], Sandesh Akre[2], Dr. M.Meena[1]

[1]Department of Electronics and Communication Engineering, [1]Vels Institute of Science, Technology and Advanced Studies, Chennai, India
[2]MET Institute of Management, Mumbai, India.
E-mail: padalasrinu@gmail.com

***Abstract*-A 5G-sub-6GHz triple band MIMO antenna is designed and analyzed on an FR-4 substrate. The transition from a simple microstrip patch antenna to the proposed rectangular slotted microstrip patch antenna is described in this article. This article consists of single-element and dual-element MIMO antennas with Ɛr of 4.3; their dimensions are 50 x 60 mm2, 50 x 120 mm2. Three resonant frequencies, 1.98 GHz, 3GHz, and 5.2GHz under sub-6GHz, are obtained by single-element and dual-element antennas. These antennas were designed using HFSS, which was also used to determine MIMO parameters, including ECC, DG, MEG, S-parameters, gain, and VSWR. S11 of single-element antennas at those resonant frequencies is -26.86 dB, -27.54 dB, and -14 dB; S11 of two-element MIMO antenna is -29.5 dB, -24.7 and -14 dB. The antenna's total gain for single and dual port MIMO is 3.39dBi and 6.074 dBi. This rectangular slotted microstrip patch antenna is suitable for various applications, such as FWA systems operating at 3 GHz frequency and 5.2 GHz high-bandwidth activities like cloud computing, video streaming, and mission-critical communications. It can also support future advancements in Wi-Fi and 5G technology.**

***Index Terms*- Return Loss, 5G, Rectangular slotted MPA (Microstrip patch antenna), High- Isolation, gain, and low VSWR.**

I. INTRODUCTION

Current microstrip technology in the field of antenna suffers from co-channel interference, a significant data rate in the channel capacity and. durability when a single antenna element is used. MIMO antennas or multiple antennas are a common solution to the aforementioned problems.High diversity performance is achieved by a MIMO antenna operating at sub-6 GHz with π-shaped circular patches that offer circular polarisation for wireless applications [1]. A MIMO antenna with revolving circular stepwise patch is built at sub-6GHz using mushroom EBG structures [2].In order to minimize mutual coupling and interfering bands, a PIFA operating in the UWB range employs techniques such as orthogonal polarisation and DGS. Strong isolation is made feasible by ground-mounted meshed stripped metal and triangular slots, and Pi-type radiators placed at a distance of 0.075-0.180 with an 180^0 spatial orientation offer impedance bandwidth for ultra-wideband applications [3, 4]. For two band applications, using CLL enhances isolation at the lower band, while complementary CLL in the ground plane improves isolation at the higher frequency band. L-shaped slotted filters are used on microstrip slot antennas with an impedance bandwidth of 2.930–20.0 GHz to eliminate WLAN and INSAT/super-extended C-band. In this instance, isolation is improved by making use of an L-shaped ground feature [5-7]. Small size uniplanar EBG reduces the coupling between the two patches in a MIMO system, as mentioned [8, 9]. A MIMO antenna with two triangle-shaped patches and a ground composed of a funnel-shaped patch connected by two triangles provides improved isolation between two radiating components. By using quasi self-complementary circular patches, UWB bandwidth is achieved. Isolation is achieved by etching the Hilbert fractal into the ground [10]. An antenna consisting of four triangular monopole MIMO antennas that radiate in different directions can neutralize ring topologies and reduce diversity performance.

The isolation between two 25 x 45 mm^2 compact

INTERNATIONAL JOURNAL OF MICROWAVE AND OPTICAL TECHNOLOGY,
VOL.19, NO.6, NOVEMBER 2024

hexagon-shaped ring monopoles positioned in opposition to each other is improved by a circular-arc ground. The Quadric-Koch Island fractal, which has dimensions of 82 x 40 x 0.80 mm^3 and is printed on FR4, is used to miniaturise patch sizes. The Sierpinski knop fractal is utilised to minimize the radiating patch's size while preserving the 0.11 λ_0 spacing between the UWB-MIMO antenna's four elements. This design supports six operational bands. A dual polarised MIMO antenna for WiMAX/WLAN bands that functions in the UWB spectrum generates both circular and linear polarisation [11–15]. Notched band features are additionally provided by an integrated two $\lambda/4$ strip resonator, a modified L-shaped stub, and ground-based CSRRs [16]. Millimetric band reflector array antennas have been developed for mobile applications [17]. For Internet of Things applications, a substrate integrated frequency selective surface antenna has been created using CST Microwave Studio [18]. For applications requiring global positioning systems, a Low-Profile Electrically Small Antenna with a Circular Slot has been constructed with ka<1 [19]. A tiny multiband hybrid rectangular DRA is one of the various dielectric resonator antennas that have been developed for use in various wireless communication applications [20]. A tiny, electrically compact antenna with split ring resonators has been created for RFID applications [21]. A low-profile dual band electrically tiny antenna has been designed for RFID applications [22]. A small electronically serrated rectangular patch antenna has been designed for RFID applications [23]. The optimisation of a single element antenna design is followed by the replication of that antenna geometry in both the horizontal and vertical orientations in order to design two and four elemental MIMO antennas. S-characteristics and other MIMO antenna parameters were measured using the ECC (Envelope Correlation Co-efficient) and DG (Diversity Gain) techniques, and all of the results are consistent with the values provided in [24].A single element antenna design followed by the replication of that in both horizontal and vertical directions in order to obtain two element and four element antennas [25].

In the proposed design circular slots are placed by the incorporation of circular slots in antenna design offers numerous advantages, including enhanced bandwidth, multiband performance, size reduction, improved impedance matching, omnidirectional radiation, and support for circular polarization. These benefits make circular slots ideal for a wide range of applications in modern communication systems, such as mobile devices, Wi-Fi, satellite communication, and IoT devices. Circular slots also provide flexibility in design, enabling engineers to optimize antennas for specific requirements like frequency reconfigurability and polarization control.

This paper presented the modelling and experimental investigation of a single-element and dual-element rectangular slotted MIMO antenna. In order to design two element MIMO antenna, the optimisation of a single element antenna design is followed by the replication of that antenna geometry in horizontal direction. MS2037C Anritsu Combinational Analyser was used to measure antenna parameters such as S_{11}, VSWR, gain, radiation pattern and MIMO parameters like MEG, ECC and DG. A close understanding between the measured and simulated results has been observed.

This article is organized as follows. Section 2 illustrates the evolution of a single element antenna from a simple microstrip patch antenna (MPA).The performance of the basic antenna configurations and other MIMO diversity parameters are presented in section 3. Consequently, concluding the article with section 4

II. ANTENNA DESIGN METHODOLOGY

This design approach covers the several stages involved in designing a MIMO antenna, with detailed analysis on the design, materials and dimensions of the antenna. A parametric analysis of the antenna at every stage of its evolution,

INTERNATIONAL JOURNAL OF MICROWAVE AND OPTICAL TECHNOLOGY,
VOL.19, NO.6, NOVEMBER 2024

MEG and ECC, is also presented in the article.

A microstrip transmission line with a characteristic impedance of 50Ω and defected ground is used to feed the rectangular microstrip antenna. The patch antenna's measurements are determined for sub-6 GHz 5G communication applications, and it takes up 29.4 x 38 x 1.6 mm³ of space. To remove the resonant frequencies over 6GHz, complementary SRRs were incorporated into the design. The dimensions that were utilised while designing the rectangular slotted MPA is represented in table 1. Fig 1 represents the simulated design and photograph of the rectangular slotted MPA.

The calculation of antenna parameters primarily depends on the following equations, where the length and width are inversely proportional to the frequency, as demonstrated in Equations (1)–(5).

The width and length of the patch at speified resonant frequencies represented by

$$W_p = \frac{c}{2f_r\sqrt{\frac{\epsilon_{r+1}}{2}}} \quad (1)$$

$$L = \frac{C}{2f_r\sqrt{\varepsilon_{reff}}} - 2\Delta l \quad (2)$$

ϵ_{reff} is the effective dielectric constant.

$$\varepsilon_{reff} = \frac{\varepsilon_r + 1}{2} + \frac{\varepsilon_r - 1}{2}\left[1 + [\frac{12h}{W_p}]\right]^{-1/2} \quad (3)$$

$$\Delta l = 0.412h\frac{(\varepsilon_{reff} + 0.03)(w + 0.26h)}{(\varepsilon_{reff} - 0.258)(w + 0.8h)} \quad (4)$$

where ∇L is the Extension in length due to fringing effect

The Radius of circular resonator (R_1, R_2) can be obtained by

$$f_r = \frac{c}{2\pi R\sqrt{\epsilon_{reff}}} \quad (5)$$

Where R is the radius of the circular patch

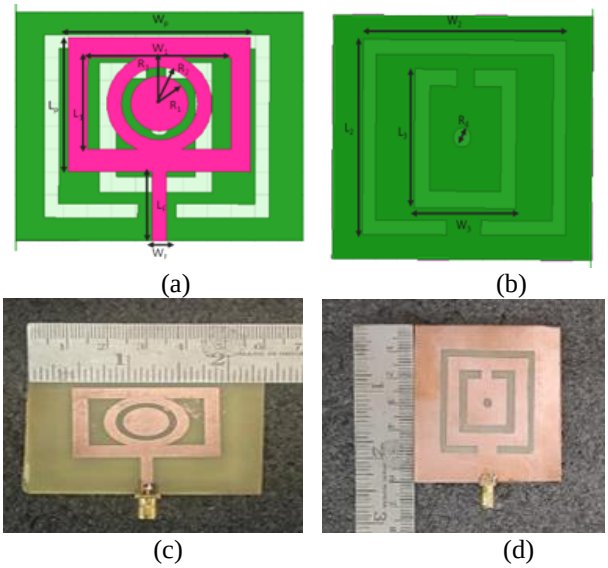

(a) (b) (c) (d)

Fig 1: Rectangular slotted MPA (a) Top view (b) Bottom view(c) Fabricated MPA from Top plane (d) Fabricated MPA from Bottom plane

Table 1: Dimensions for Rectangular slotted MPA

S. No	Variables	Values (mm)
1	Patch Length (LP)	29.4
2	Patch Width (WP)	38
3	Feedline length (LF)	15.3
4	Feedline width (WF)	3
5	Length (L1)	20
6	Width (W1)	30
7	Length (L2)	40
8	Width (W2)	40
9	Length (L3)	25
10	Width (W3)	23.5
11	Radius of circle (R1)	11
12	Radius of Circle (R2)	8
13	Radius of circle (R3)	6
14	Radius of Circle (R4)	2

The equivalent circuit of proposed antenna as shown in Fig.2 The series LC is used for impedance matching, filter tuning and improving overall performance of the antenna. Similarly, parallel LC in the equivalent circuit is used for excel at frequency rejection, bandwidth control, and miniaturization. Together, they enable antennas to operate efficiently over the desired frequency range, making them vital components in modern communication systems.

The equivalent circuit in antenna design simplifies the complex electromagnetic interactions into a manageable electrical model, allowing engineers to analyze, design, and optimize antennas efficiently.

This approach is essential for ensuring proper impedance matching, analyzing resonance and bandwidth, understanding radiation efficiency, and ultimately improving antenna performance in real-world applications.

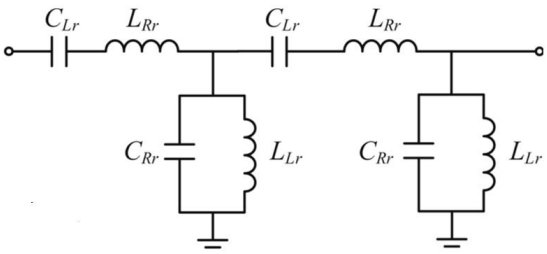

Fig. 2. Equivalent circuit of the proposed antenna

The iterative design of a rectangular slotted MPA is shown in Fig 3. The defected MPA was designed to resonate at 1.98 GHz, 3 GHz, and 5.2 GHz 5G-Sub-6GHz applications. But since the antenna isn't resonating at those frequencies, the design had to be modified in order to get the desired results for those particular applications. At first 20mm x 30mm has been subtracted from the microstrip rectangle. The first iteration antenna is resonating at 2.9 GHz with a return loss of -10.9dB, 3.2 GHz with a return loss of -13dB, 4 GHz with a return loss of -31dB, 5.2 GHz with a return loss of -20.3dB, 5.99 GHz with a return loss of -25dB and 7.05 GHz with a return loss of -20.5 dB. In iteration 2 three circles with a radius of 11mm, 6mm and 2mm have been united with the iteration 1 antenna. Iteration 2 antenna is resonating at 3.2 GHz, 4.2 GHz, 6.2 GHz and 6.9 GHz with a return loss of -22dB, -15dB, -12dB and -16dB respectively. We have used complimentary SRRs measuring 3 x 40 mm2 and 41 x 3 mm2 in the ground. After that a circle with a radius of 2 mm is removed from the ground. The results of the third iteration show that the resonance at 1.98 GHz with a return loss of -26.86 dB, 3.0 GHz with a return loss of -27.54 dB, and 5.2 GHz with a return loss of -14 dB. Since our rectangular slotted MPA resonates at our desired resonating frequencies, it is our final iteration.

The MS2037C Anritsu Combinational Analyser can be utilised to measure radiation pattern and gain using the measuring setup of an anechoic chamber, as shown in Fig 4.

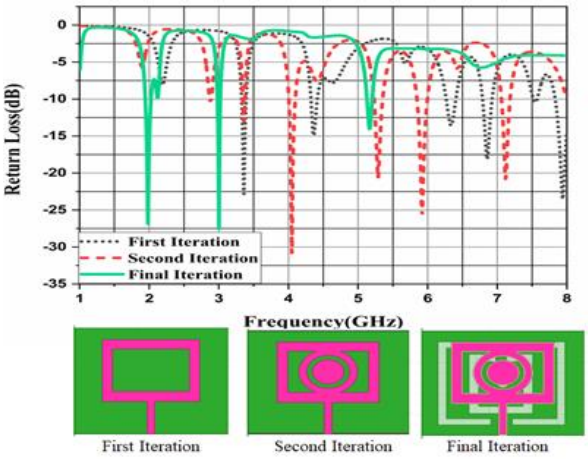

Fig 3: Evolution of rectangular slotted MPA

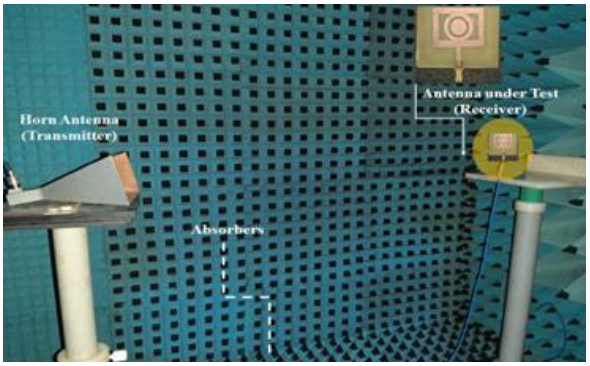

Fig 4: Radiation pattern Measurement of Rectangular slotted MPA using Anechoic chamber.

The single element antenna is replicated along the horizontal axis in order to attain dual-element rectangular slotted MIMO antenna. The MIMO antenna's numerous elements allow it to provide several data streams for simultaneous large-scale data transmission and reception. Multiple directions are used to receive the signals, which enhances overall performance and signal quality. Therefore, a MIMO antenna technology is the best option to achieve these goals.The inter-element spacing of λ/4 was maintained between the two elements in order to attain the spatial

diversity depicted in Fig.5. The fact that no further isolation techniques were required increases the complexity of the antenna's design. The dimensions of this dual element antenna are 50 x 120 x 1.6 mm^3. Fig 5 shows the dual-element defective L-shaped microstrip patch MIMO antenna.

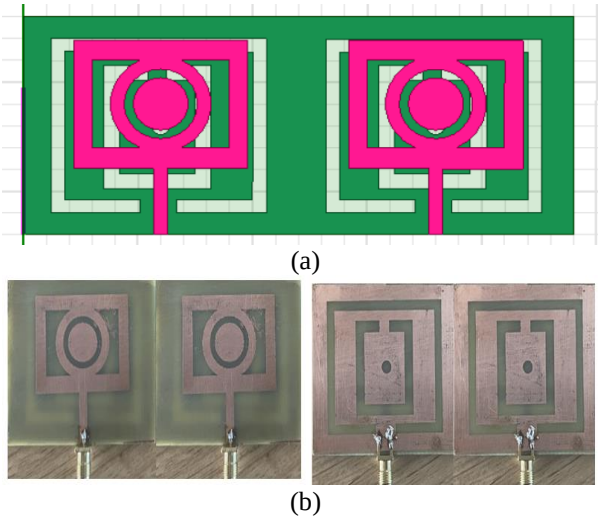

(a)

(b)

Fig.5: Dual-element Rectangular slotted MIMO antenna (a) Simulated (b) Manufactured design and (c) Fabricated design of 2X2 MIMO antenna.

III. RESULTS & DISCUSSIONS

This section is divided into subsections that provide a thorough description of the simulated results and conclusions that may be drawn from them.

A. Single-Element rectangular slotted MPA

As shown in Fig 1, the final iteration antenna is fabricated using FR4 epoxy material. The substrate is used to connect the radiating top and bottom planes, and SMA connector is used to attach the bottom and top planes.

Simulated and fabricated S_{11} of the rectangular slotted MPA is represented in Fig.6. Single element rectangular slotted MPA resonates at 1.98 GHz with a return loss of -26.86 dB, 3.0 GHz with a return loss of -27.54 dB and 5.2 GHz with a return loss of -14 dB as shown in figure 5. Fabricated antenna resonates at 1.98 GHz with a return loss of -25dB, 3.0 GHz with a return loss of -26dB and 5.2 GHz with a return loss of -13dB. Variation between the simulated and measured results may be observed because of the connector losses, cable losses as well as the calibration errors.

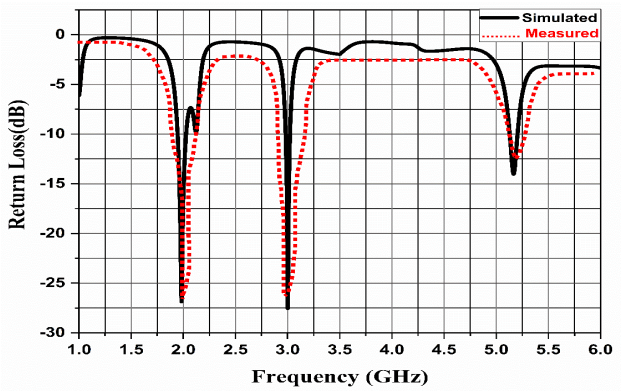

Fig.6: S_{11} of the rectangular slotted MPA

The ideal value of VSWR requires a range of 0–2. Fig.7 illustrates the measured and simulated VSWR values for the single element antenna, which are 1.10 at 1.9 GHz, 1.18at 3 GHz and 1.5 at 5.2 GHz, respectively. To measure the radiation pattern, the antenna is set up in an anechoic chamber. The radiation pattern of the implemented design in the E- and H-plane at 1.98GHz, 3.0 GHz and 5.2GHz is shown in Fig.8.There is good co-pol and cross-pol difference in broadside direction in both the major plane (E&H), i.e., more than 20 dB at all three frequency bands. Fig 8 shows that for the two resonant frequency bands, the radiation patterns in the E and H-plane are omni directional. The radiation properties of the model are good. The surface current distribution for 1.98 GHz, 3.0 GHz, and 5.2 GHz is shown in Fig.9 (a), (b), and (c), respectively. The antenna's performance and efficiency can be obtained from the current distribution on the device. We can infer from looking at Fig.9 that the electric current is dispersed symmetrically throughout the patch and feedline, indicating the efficiency of the antenna.

The three-dimensional gain of the single-element rectangular slotted MPA, which has a maximum gain of 3.39 dBi recorded, is shown in Fig.10.

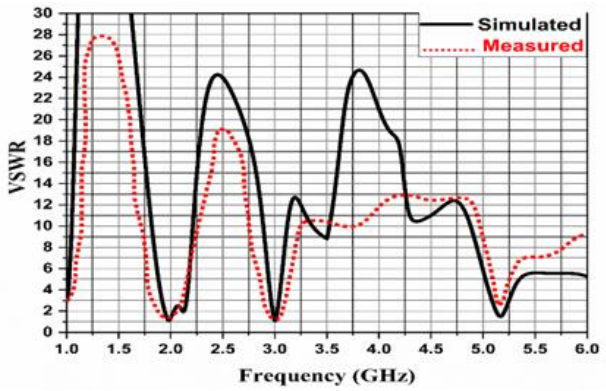

Fig.7: VSWR of the rectangular slotted MPA

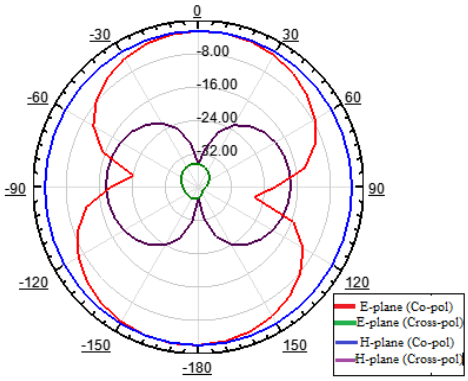

(a)

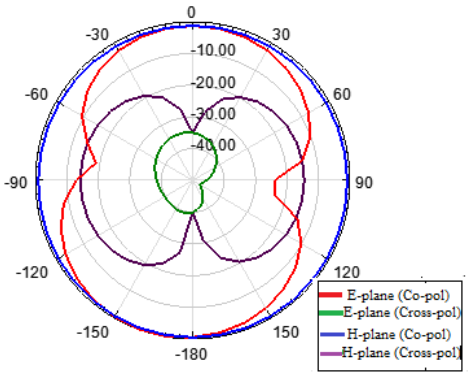

(b)

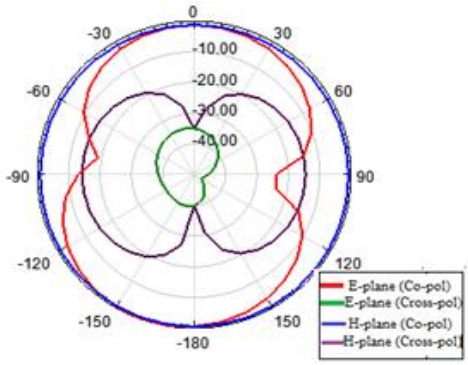

(c)

Fig.8: Simulated and Measured radiation pattern of the rectangular slotted MPA(a) at 1.98 GHz
(b) at 3.0 GHz (c) at 5.2 GHz.

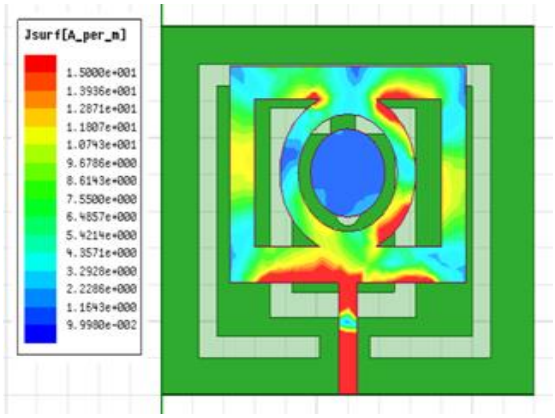

(a)

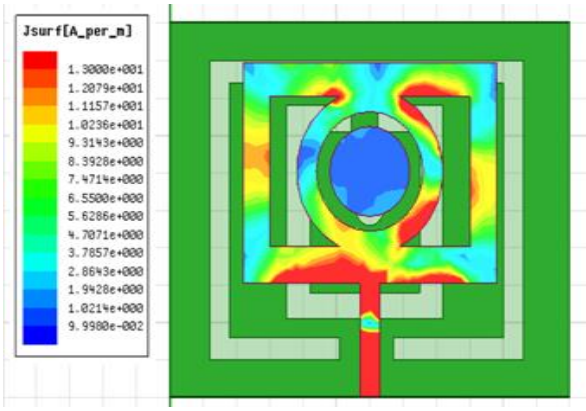

(b)

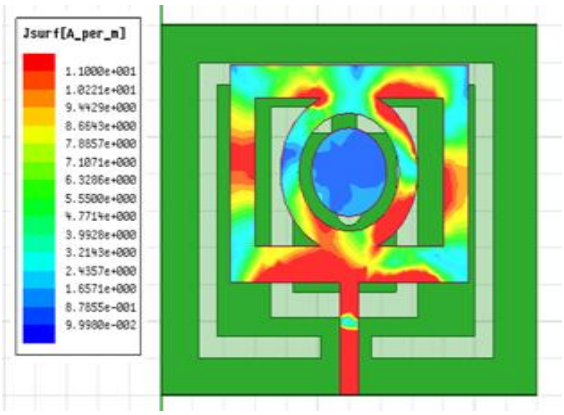

(c)

Fig.9: Surface Current Distribution of rectangular slotted MPA (a) 1.98 GHz (b) 3.0 GHz (c) 5.2GHz

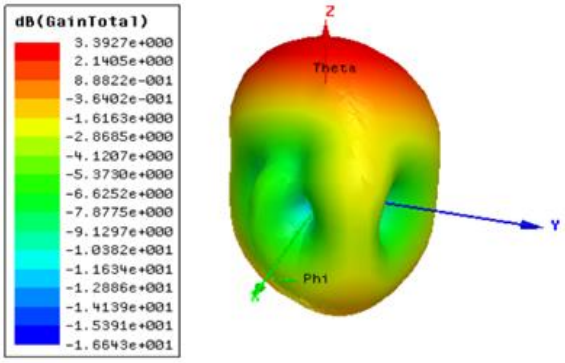

Fig.10: 3D gain of the rectangular slotted MPA

B. Dual-Element Rectangular slotted MIMO Antenna

Accuracy and data throughput are the two major concerns of 5G. It is believed that MIMO antenna technology is the best option for enhanced performance. Because of its many components, the MIMO antenna can transmit and receive a large amount of data in several data streams at In addition to other MIMO antenna characteristics like ECC and DG and MEG this part evaluated the performance of a dual element rectangular slotted microstrip patch MIMO in terms of S_{11}, transmission co-efficient, VSWR, radiation pattern, gain, and surface current distributions. The simulated and fabricated S_{11} of the dual-element rectangular slotted MIMO antenna is shown in Fig.11. The simulated and fabricated $S_{12}$of the dual-element rectangular slotted MIMO antenna is shown in Fig.12the same time. The signal coming in from different directions degrades both the overall performance and the quality of the signals. For these purposes, MIMO antenna technology is the most suitable choice.

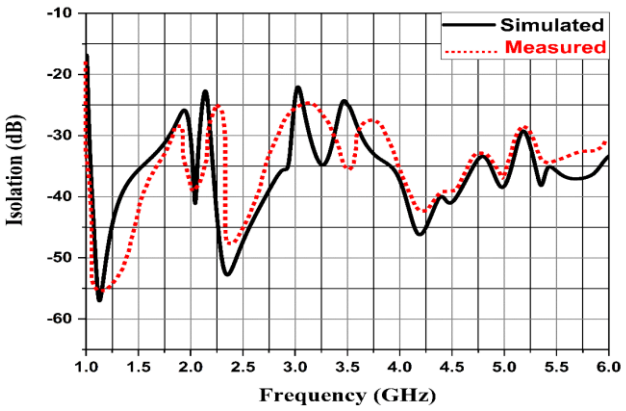

Fig.11:S_{11} of the Dual-element rectangular slotted MicrostripMIMO antenna

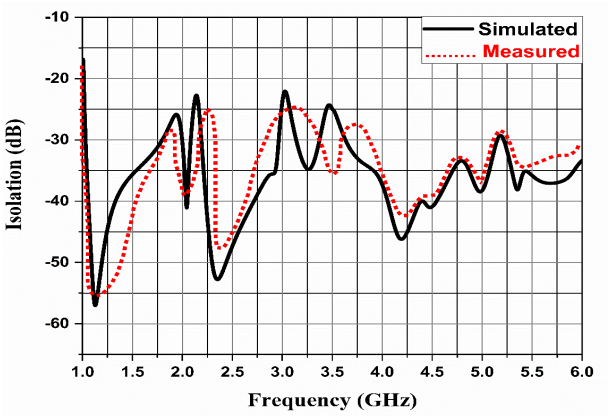

Fig.12:S12 of the Dual-element rectangular slotted Microstrip MIMO antenna

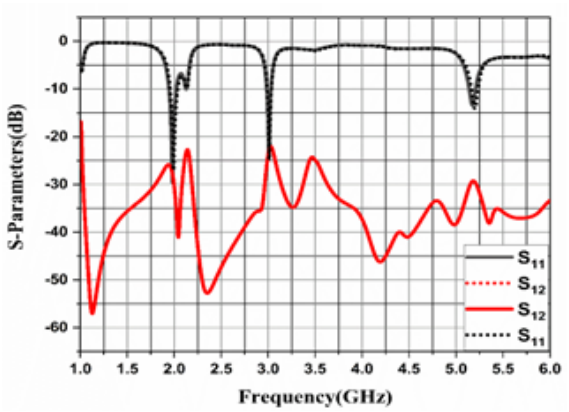

Fig.13: S-Parameters of the Dual-element rectangular slotted MicrostripMIMO antenna

While Fig.11 shows S_{11} for the two port MIMO antenna and Fig. 12 shows S_{12} for the dual port MIMO antenna, Fig.13 shows all of the S-Parameters. The simulated antenna resonates at 1.98 GHz with a return loss of -29.5 dB,3.0 GHz with a return loss of -24.7dB, and at 5.2 GHz with a return loss of -14 dB. The fabricated design resonates at 1.98 GHz with a return loss of -28.8 dB, 3.0 GHz with a return loss of -24 dB, and 5.2 GHz with a return loss of -14dB. The simulated and measured VSWR are 1.10at1.9 GHz, 1.18at 3 GHz and 1.5 at 5.2 GHz, as shown Fig.14. VSWR of the rectangular slotted MIMO antenna is shown in Fig.15. This shows that the antenna is operating at a satisfactory level. The radiation pattern and surface current distribution of the two-port antenna for the 1.98 GHz, 3.0 GHz, and 5.2 GHz bands are depicted in Fig.16 and 17, respectively. Fig.16 displays the two-port MIMO antenna's measured and calculated radiation patterns. It shows the radiation pattern of the implemented design in the E- and H-plane at 1.98 GHz, 3.0 GHz, and 5.20GHz. There is good co-pol and cross-pol difference in broadside direction in both the major plane (E&H), i.e., more than 20 dB at all three frequency bands. Fig.17 illustrates, The surface Current Distribution of rectangular slotted MIMO antenna at 1.98 GHz, 3.0 GHz, and 5.20GHz.. The three-dimensional gain of the dual-elemental defective L-shaped MPA is shown in Fig 18.

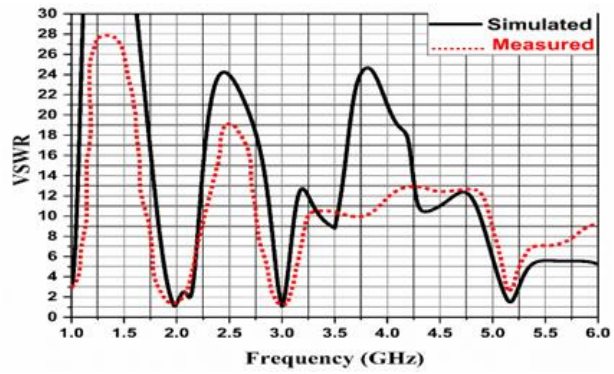

Fig.14: VSWR of the dual-element rectangular slotted MIMO antenna

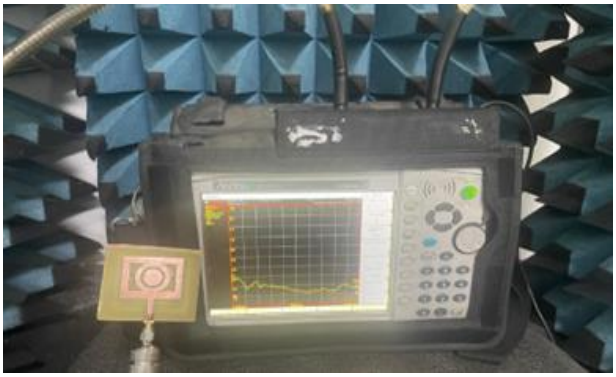

Fig.15: Measurement of VSWR using MS2037C Anritsu Combinational Analyzer

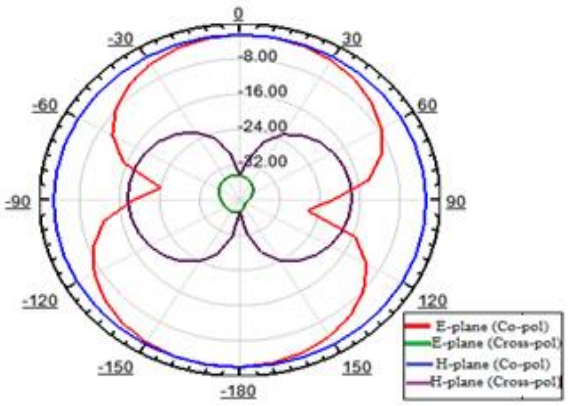

(a)

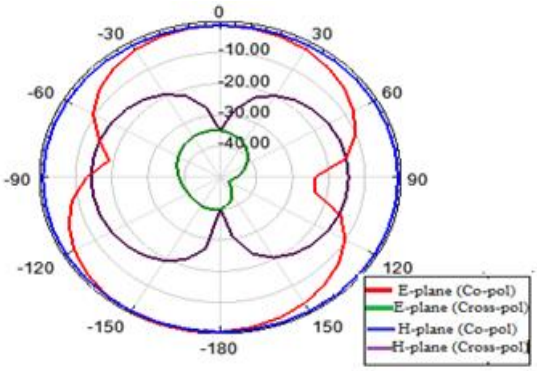

(b)

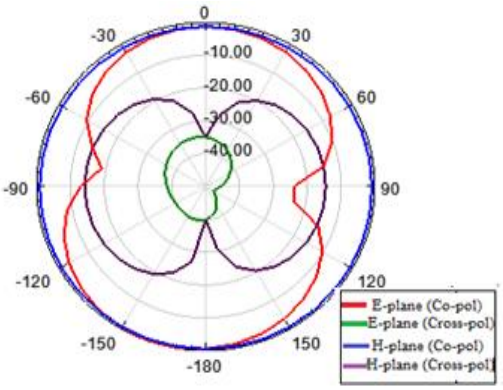

(c)

Fig.16: Simulated and Measured radiation pattern of the dual-element rectangular slotted MIMO antenna (a) at 1.98 GHz (b) at 3.0 GHz (c) at 5.2 GHz

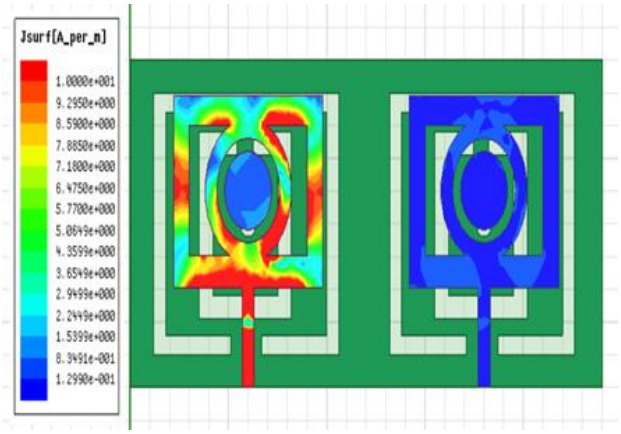

(a)

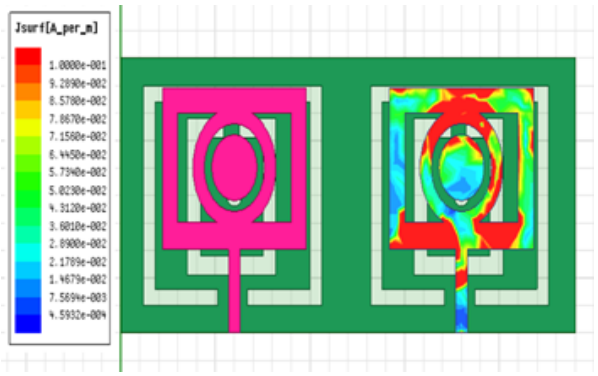

(b)

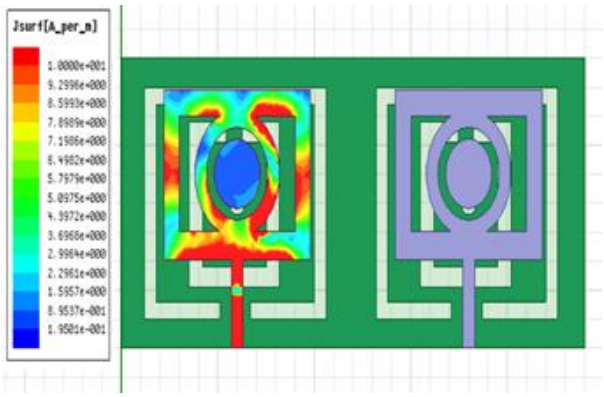

(c)

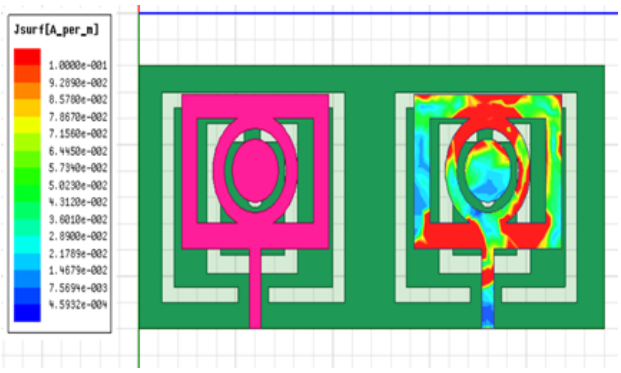

(d)

INTERNATIONAL JOURNAL OF MICROWAVE AND OPTICAL TECHNOLOGY,
VOL.19, NO.6, NOVEMBER 2024

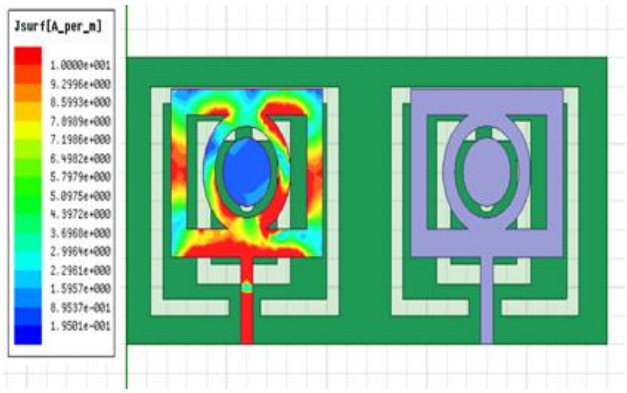

(e)

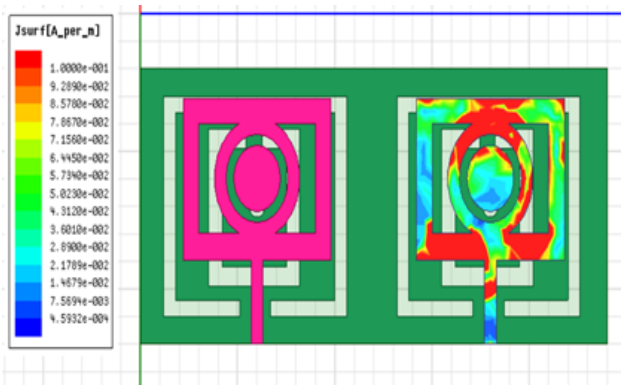

(f)

Fig.17: Surface Current Distribution of rectangular slotted MIMO antenna (a, b) 1.98 GHz (c, d) 3.0 GHz (e, f) 5.2GHz

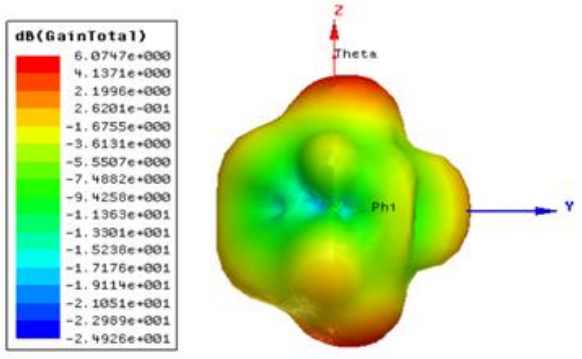

Fig.18: 3D gain of the dual-element rectangular slotted MIMO antenna

C. . Analysis of MIMO Diversity Parameters

ECC, DG and MEG are used to ensure that the designed antenna meets the requirements stated in [15–19] while measuring the effectiveness of MIMO diversity parameters.

One of the most important parameters for assessing a MIMO antenna's performance is its ECC. It establishes the relationship between the design's neighbouring elements. ECC has a range of values from 0 to 0.5, with 0 being its usual value. There are two methods for computing its: radiation pattern or S-Parameters

This is the ECC formula based on the S-Parameters.

$$\rho_e = \frac{|S_{11}^* S_{12} + S_{21}^* S_{22}|^2}{(1-|S_{11}|^2-|S_{21}|^2)(1-|S_{22}|^2-|S_{12}|^2)} \quad (6)$$

$$ECC_{qp} = \frac{\left|\int_0^{2\pi}\int_0^{\pi}\left(E_{\theta p}^* E_{\theta q} P_\theta XPR + E_{\varphi p}^* E_{\varphi q} P_\varphi\right)d\Omega\right|^2}{\alpha \times \beta} \quad (7)$$

$$\alpha = \int_0^{2\pi}\int_0^{\pi}\left(E_{\theta q}^* E_{\theta q} P_\theta XPR + E_{\varphi q}^* E_{\varphi q} P_\varphi\right)d\Omega \quad (8)$$

$$\beta = \int_0^{2\pi}\int_0^{\pi}\left(E_{\theta p}^* E_{\theta q} P_\theta XPR + E_{\varphi p}^* E_{\varphi q} P_\varphi\right)d\Omega \quad (9)$$

A MIMO antenna's quality and dependability are indicated by its diversity gain. It is computed by taking the ECC values into account. Ten dB is the best number for it.

$$DG = 10 \times \sqrt{1 - \left|ECC_{qp}\right|^2)} \quad (10)$$

The ECC and DG of a dual-port MIMO antenna are shown in Fig.19. The ECC and DG values of this specific antenna are within the optimal range, suggesting that the MIMO antenna is appropriate for the intended purpose.

INTERNATIONAL JOURNAL OF MICROWAVE AND OPTICAL TECHNOLOGY,
VOL.19, NO.6, NOVEMBER 2024

An additional parameter to take into account when determining the antenna's diversity is mean effective gain. The ratio of the mean incident power to the mean received power is how it is known. The following formula is used to calculate the MEG. There shouldn't be a significant variation in the gain produced by various antenna components because the MIMO antenna is made up of identical antenna elements. For MEG, 0 dB is the optimum theoretical limit. Table 2 indicates that the variance is within allowable bounds, making the device more appropriate for MIMO communications. The crucial factor known as the mean effective gain in a fading scenario is the mean received power. The numerically computed numbers are displayed in Table 2. The practical value recommended for the proposed antenna is -3 dB less than or equal to MEG (dB) -12 for optimal performance. As a result, all MIMO configurations' MEG values were confirmed.

Table 2: The values of mean effective gain (MEG) at frequency sweep

Operating Frequency (GHz)	1 Antenna	2 Antenna
1	6.9	6.4
1.5	7.1	6.4
2	8.4	8.3
2.5	6.7	6.4
3	7	6.5
3.5	6	6.6
4	9	8.9
4.5	7	8.2
5	6.5	7
5.5	6.7	6.6
6	6.7	6.4

Table 3: A table comparing the proposed MIMO design to the models that are currently in use

Ref. No	Element	Bandwidth	Dimensions	Return Loss	VSWR	Gain	ECC	DG
[1]	1	1.5-7.0GHz	60×97mm2	-18dB	<2	----	----	------
	2	1.5-6.5GHz	97×60mm2	-18.5dB	<2	3dB	0.2	9.9
	4	1.5-3.8,4.2-6.2GHz	110×120 mm2	-18.5dB	<2	3.1dB	0.2	-----
[3]	1	3.6-8.3GHz	37×40mm2	-30dB	<1.8	----	----	-----
	2	3.6-8.3GHz	40×80mm2	-28dB	<1.8	-----	-----	-----
	4	3.6-8.3GHz	180×180mm2	-20dB	<1.8	-----	0.2	9.9
[4]	4	3.6GHz	120×60mm2	-28dB	<2	----	-----	----
[5]	4	2.7GHz	130 × 190mm2	-25dB	<1.5	----	-----	-----
[6]	1	3.5–5.4 GHz	20×20mm2	-24dB	1.8	-----	------	-----
	4	3.5–5.8 GHz	180×180mm2	-16dB	1.3	2.4	----	----
[7]	4	1.7–7.2GHz	110 ×100mm2	-21dB	1.5	2.0	0.025	----
[8]	4	2.45GHz	100×120 mm2	-35dB	1.8	1.4	0.002	---
[9]	4	2.4GHz	186×188mm2	-30dB	1.2	1.6	0.12	7.95
[10]	4	2.4-2.48GHz	100×100mm2	-28dB	1.5	1.5	0.2	----
[11]	4	3.6-5.3GHz	100×95mm2	-20dB	1.82	2.1	0.5	----
proposed design	1	1.98GHz 3.0GHz 5.2GHz	50×60mm2	-26.86dB -27.54dB -14dB	<1.5	3.39	----	-----
	2	1.98GHz 3.0GHz 5.2GHz	50 × 120 mm2	-29.5dB -24.7dB -14dB	<1.2	6.7	0.006	9.99

INTERNATIONAL JOURNAL OF MICROWAVE AND OPTICAL TECHNOLOGY,
VOL.19, NO.6, NOVEMBER 2024

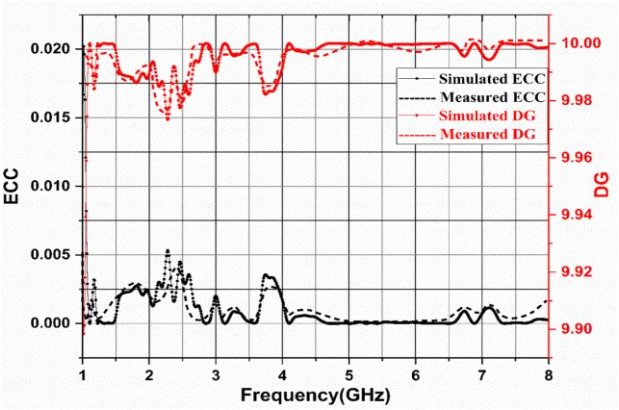

Fig.19: ECC and DG for dual-port MIMO antenna

A comparison of the rectangular slotted MIMO antenna and several other sub-six GHz MIMO antennas is shown in Table 3. Dimensions, diversity gain, return loss, gain, and envelope correlation coefficient are all compared. It is demonstrated that the suggested antenna performs better and is smaller than the other antennas. MIMO antennas have been proposed in earlier research [8, 9, 10, 17, 18, and 19], however they are larger and offer less gain than the suggested antenna. One economical method of increasing manufacturing efficiency is chemical etching of microstrip devices.

IV. CONCLUSION

A dual elemental MIMO antenna is proposed in this article which describes in detail about the designing of the antenna from a basic microstrip antenna to the proposed rectangular slotted MIMO through various modifications to resonate at the desired frequency. This proposed single antenna resonates at 1.98 GHz, 3.0 GHz, and 5.2 GHz frequencies with -26.86 dB return loss and -27.54 dB return loss and -14 dB return loss respectively. To improvise the data rate, the existing design was modified to design a two- port MIMO antenna. These antennas resonate at 1.98 GHz, 3.0 GHz, and 5.2 GHz frequencies with -29.5 dB return loss and -24.7 dB return loss and -14 dB return loss respectively. The antenna has an isolation of -23dB at 1.98 GHz, -30 dB at 3.0 GHz and -35 dB at 5.2 GHz. MIMO diversity parameters such as ECC is less than 0.003 and DG is nearly 10 dB are included in addition to S-Parameters. Many applications that need cellular connection can benefit from this architecture, including surveillance, medical care, smart homes, industrial automation, and agriculture.

REFERENCES

[1] Malaisamy K, Santhi M, Robinson S . “Design and analysis of 4 × 4 MIMO antenna with DGS for WLAN applications”, *International Journal of Microwave and Wireless Technologies*. Vol. 13, pp. 979 – 985, Nov. 2021.

[2] Goldsmith, A., Jafar, S.A., Jindal, N. and Vishwanath, S. “Capacity Limits of MIMO Channels”, *IEEE Journal on Selected Areas in Communications*, Vol. 21, pp. 684-702, Jun 2003.

[3] Khan MS, Shafique MF, Naqvi A, Capobianco AD, Ijaz B and Braaten BD, “A miniaturized dual band MIMO antenna for WLAN applications” *IEEE Antennas and Wireless Propagation Letters*., Vol .14, pp. 958–961, Jan. 2015.

[4] Abdulla MA and Ibrahim AA. “Compact and closely spaced meta material MIMO antenna with high isolation for wireless applications”, *IEEE Antennas and Wireless Propagation Letters*, Vol. 12, pp. 1452–1455, Nov. 2013.

[5] Thummaluru SR and Chaudhary RK. “Mu-negative Meta material filter-based isolation technique for MIMO antennas”. *ELECTRONICS LETTERS IET*,Vol. 53, pp. 644-646, May 2017.

[6] Jusoh M, Jamlos MF, Kamarudin MR and Malek F, “A MIMO antenna design challenges for UWB application”, *Progress in Electromagnetic Research* B, Vol. 36, pp. 357-371, 2012.

[7] Palandoken M,Grede A Henke H. “Broadband micro strip antenna with left-handed Meta material”,. *IEEE Antennas and Wireless Propagation Letters.* Vol. 57, pp. 1468-1471, Feb 2009.

[8] Nordin MAW, Islam MT and Misram N. “Design of a compact ultra-wideband meta material antenna based on the modified split ring resonator and capacitively loaded strips unit cell”, *Progress in Electromagnetic Research Vol*. 136,pp. 157-173, Jan. 2013.

[9] Nandi S and Mohan A. “A compact dual band MIMO slot antenna for WLAN application”, *IEEE Antennas and Wireless Propagation Letters,* Vol.16, pp.2457-2460, Jul.2017.

[10] Mallahazedh AR, ES’haghi S and Alipour A. “Design of an E shaped MIMO antenna using two algorithms for wireless application at 5.8 GHz”, *Progress in Electromagnetic Research* , Vol. 90,pp. 187-203, 2009.

[11] Chou HT, Cheng HC, Hsu HT and Kuo LR. “Investigation of isolation improvement techniques for multiple input multiple output WLAN portable terminal applications”, *Progress In Electromagnetic Research,* Vol.85, pp. 349-366, Jan 2008.

[12] YU XH, Wang L, Wang HG, Wu XD and Shang YH. "A novel multiport matching method for maximum capacity of an indoor MIMO system". *Progress in Electromagnetic Research*, Vol. 130, pp. 67-84, Jul. 2012.
[13] Kim SH, Lee JY, Nguyen TT and Jang JH. "High performance MIMO antenna with 1-D EBG ground structures for handset applications", *IEEE Antennas and wireless Propagation Letters*, Vol. 12, pp. 1468-1471, Nov. 2013.
[14] Krairiksh M, Keowsawat P, Phongcharoenpanich C and Kosulvit S. "Two probe excited circular ring antenna for MIMO application", *Progress in Electromagnetic Research*, Vol. 97, pp. 417–431, Oct. 2009.
[15] Parchin NO, Al-Yasir YIA, AliAH, ElferganiI SSA, Noras, JM, Rodriguez J and Abd-Alhameed RA. "eight element dual polarized MIMO slot antenna system for 5G smart phone applications. *IEEE Access*, Vol. 7, pp. 15612–15622, Jan. 2019.
[16] Barani IRR and Wong K-L. "Integrated inverted-F and open-slot antennas in the metal-framed smart phone for 2*2 LTE LB and 4*4 LTEM/HBMIMO operations", *IEEE Transactions on Antennas and Propagation*, Vol. 66, pp. 5004–5012, Oct. 2018 .
[17] Yao Huan Gong, "Multiple input multiple out of smart antenna technology," *ZTE Technology*, vol. 6, pp. 19–21, 2002.
[18] Li Gang Ren and Mei Song, "MIMO technology in mobile communication [J]", *Modern Telecommunication technology*, vol.1, pp. 42–45, 2004.
[19] G. J. Foschini, "Layered space-time architecture of wireless communication in a fading environment when using multi element antennas," *Bell Labs Technical Journal*, vol. l, no. 2, pp.41–59, 1996.
[20] G. J. Foschini, "On limits of wireless communications in a fading environment when using multiple antennas," *Wireless Personal Communications*, vol. 6, no. 3, pp. 311–335, 1998.
[21] IMT Vision—Framework and Overall Objectives of the Future Development of IMT for 2020 and beyond, document Recommendation ITU-R M.2083-0, pp. 1–21. 2015.
[22] S. Kumar, A. S. Dixit, R. R. Malekar, H. D. Raut and L. K. Shevada, "Fifth Generation Antennas: A Comprehensive Review of Design and Performance Enhancement Techniques", *IEEE Access*, vol. 8, pp. 163568-163593, 2020.
[23] D. Sarkar and K. V. Srivastava, "Four Element Dual-band Sub-6 GHz 5G MIMO Antenna Using SRR-loaded Slot-Loops," *2018 5th IEEE Uttar Pradesh Section International Conference on Electrical, Electronics and Computer Engineering (UPCON)*, Gorakhpur, India, pp. 1-5, Nov. 2018.
[24] A. L. Swindlehurst, E. Ayanoglu, P. Heydari, and F. Capolino, "Millimeter-Wave massive MIMO: The Next Wireless Revolution," *IEEE Communications Magazine*, Vol. 52, pp. 56-62, Sep. 2014.
[25] T. Tuovinen, N. Tervo and A. Parssinen, "Analysing 5G RF System Performance and Relation to Link Budget for Directive MIMO", *IEEE Transactions on Antennas and Propagation*, vol. 65, no. 12, pp. 6636-6645, Dec. 2023.